Accepted Manuscript

Precision of Bone Mineral Density Measurements Around Total Ankle Replacement Using Dual Energy X-ray Absorptiometry

Carmelo Messina MD , Federico Giuseppe Usuelli MD ,
Camilla Maccario MD , Claudia Angela Di Silvestri MD ,
Salvatore Gitto MD , Maria Cristina Cortese MD ,
Domenico Albano MD , Luca Maria Sconfienza MD, PhD

PII: S1094-6950(18)30250-6
DOI: https://doi.org/10.1016/j.jocd.2019.01.006
Reference: JOCD 1109

To appear in: *Journal of Clinical Densitometry*

Received date: 26 November 2018
Revised date: 28 January 2019
Accepted date: 28 January 2019

Please cite this article as: Carmelo Messina MD , Federico Giuseppe Usuelli MD , Camilla Maccario MD , Claudia Angela Di Silvestri MD , Salvatore Gitto MD , Maria Cristina Cortese MD , Domenico Albano MD , Luca Maria Sconfienza MD, PhD , Precision of Bone Mineral Density Measurements Around Total Ankle Replacement Using Dual Energy X-ray Absorptiometry , *Journal of Clinical Densitometry* (2019), doi: https://doi.org/10.1016/j.jocd.2019.01.006

Precision of Bone Mineral Density Measurements Around Total Ankle Replacement Using Dual Energy X-ray Absorptiometry

Running Title: BMD Precision Around Total Ankle Replacement

List of authors and affiliations:

- Carmelo Messina, MD [1,2]; email: carmelo.messina@unimi.it, *ORCID ID: https://orcid.org/0000-0001-7518-5773*
- Federico Giuseppe Usuelli, MD [3]; email: fusuelli@gmail.com, *ORCID ID: https://orcid.org/0000-0003-2795-6603*
- Camilla Maccario, MD [3] email: camillamaccario@gmail.com;
- Claudia Angela Di Silvestri, MD [3] email: claudiadisilvestri@icloud.com;
- Salvatore Gitto, MD [4] email: sal.gitto@gmail.com;
- Maria Cristina Cortese, MD [5,6] email: cristinacortese1010@gmail.com
- Domenico Albano, MD [1] email: albanodomenico@icloud.com, *ORCID ID: https://orcid.org/0000-0001-7989-9861*
- Luca Maria Sconfienza, MD, PhD [1,2]; email: io@lucasconfienza.it, *ORCID ID: https://orcid.org/0000-0003-0759-8431*

1. IRCCS Istituto Ortopedico Galeazzi, Via Riccardo Galeazzi 4, 20161 Milan, Italy.
2. Dipartimento di Scienze Biomediche per la Salute, Università degli Studi di Milano, Via Carlo Pascal, 36, 20133, Milan, Italy
3. C.A.S.C.O. Piede e Caviglia - IRCCS Istituto Ortopedico Galeazzi, Via Riccardo Galeazzi 4, 20161 Milan, Italy.
4. Scuola di Specializzazione in Radiodiagnostica, Università degli Studi di Milano, Via Festa del Perdono, 7, 20122 Milan, Italy.

5. Radiologia Diagnostica e Interventistica Generale, Area Diagnostica per Immagini, Dipartimento Diagnostica per Immagini, Radioterapia Oncologica ed Ematologia, IRCCS Fondazione Policlinico Universitario A. Gemelli, Roma, Italia
6. Istituto di Radiologia, Università Cattolica del Sacro Cuore, Roma, Italia

Corresponding author:

Dr. Carmelo Messina

Address: Via Bellincione 10, 20134 Milan, Italy

Email: carmelo.messina@unimi.it

Telephone: +39 346 6707007

Acknowledgements: Authors' roles: CME contributed to study design, data acquisition, analysis and interpretation, manuscript drafting; FGU, CMA, CDS, DA, MCC and SG contributed to data acquisition and manuscript revising, LMS revised the manuscript and approved its final version.

CM is responsible for the integrity of the data analysis.

Funding Source: None.

Abstract

Introduction

Joint prosthesis survival is associated with the quality of surrounding bone. Dual-energy X-ray Absorptiometry (DXA) is capable to evaluate areal bone mineral density (BMD) around different prosthetic implants, but no studies evaluated periprosthetic bone around total ankle replacement. (TAR). Our aim is to determine the precision of the DXA periprosthetic BMD around TAR.

Methodology

Short-term precision was evaluated on 15 consecutive patients. Each ankle was scanned three times both in the posteroanterior (PA) and lateral views with a dedicated patient positioning protocol. Up to four squared ROIs were placed in the periprosthetic bone around tibial and talar implants, with an additional ROI to include the calcaneal body in the lateral scan. Coefficient of variation (CV%) and least significant change (LSC) were calculated according to the International Society for Clinical Densitometry (ISCD).

Results

The lateral projection showed lower mean CV values compared to the PA projection, with an average precision error of 2.21% (lateral scan) compared to 3.34% (PA scans). Overall, the lowest precision error was found at both “global” ROIs (CV = 1.25% on PA, CV= 1.3% on lateral). The highest CV value on PA was found at the medial aspect of talar side (ROI 3; CV= 4.89%), while on the lateral scan the highest CV value was found on the posterior aspect of talar side (ROI 2; CV = 2.99%).

Conclusions

We found very good reproducibility BMD values of periprosthetic bone around TAR, that were comparable or even better compared to other studies that evaluated periprosthetic BMD around different prosthetic implants. DXA can be used to precisely monitor bone density around ankle prostheses, despite further long-term longitudinal studies are required to assess the clinical utility of such measurements.

Keywords

Total Ankle Replacement; DXA; periprosthetic BMD; precision; metal removal

Introduction

Nowadays, hip and knee arthroplasties are considered highly successful options for the management of osteoarthritis [1]. Conversely, there is an ongoing debate between surgeons supporting the use of total ankle replacement (TAR) and those supporting ankle fusion for the treatment of end-stage ankle osteoarthritis, due to the disappointing results of first generation TAR implants [2]. After three implant generations, significant improvements have been done to implant design as well as to surgery and fixation techniques, leading to a substantial increase in the number of TAR performed every year [3].

Whatever the joint, the mainstay of longitudinal radiological evaluation of periprosthetic bone is represented by serial plain radiographs assessment, with the complement of computed tomography (CT) and magnetic resonance imaging (MRI) [4–8]. Joint prosthesis survival is associated with the quality of surrounding bone, as aseptic loosening around implants remains the most common cause for revision surgery [9]. The mechanism of asepting loosening around TAR is still poorly understood and multifactorial, with several factors related to patient’s characteristic (age, body weight) and implant design contributing to periprosthetic bone adaption and osteolysis development [9]. As a matter of fact, periprosthetic osteolysis has been reported as a common phenomenon after TAR, and early detection has been advocated due to possible implication in long-term mechanical failure compared to arthrodesis [10]. Thus, it is of great importance to accurately evaluate periprosthetic bone environment, as bone loss may not only lead to loosening of the prosthetic components, but can create difficulties during possible revision [11]. Despite plain radiographs can reliable assess the bone-prosthesis interfaces by detecting peri-implant radiolucency, the quantitative evaluation of periprosthetic bone density is unreliable [12, 13]. In fact, it is well known that bone loss on standard radiographs can be detected only when a considerable amount (usually 20-40%) has occurred [14, 15]. On the other side, dual-energy X-ray absorptiometry (DXA) with dedicated “metal-removal” software is capable to evaluate areal bone mineral density (BMD) around different prosthetic implants [16]. This imaging modality has proven to precisely measure small bone mineral changes around total hip arthroplasty (THA) and total knee arthroplasty (TKA), allowing to evaluate bone remodeling during follow-up [17–20].

In order to detect small differences between serial scans that can be considered a true biological change, BMD measurements from DXA must have good precision. According to the International Society for Clinical Densitometry (ISCD) the minimum acceptable precision (expressed as a coefficient of variation, CV) is 1.9% at the lumbar spine and 2.5% at the femoral neck, with least significant change (LSC) values of 5.3% and 6.9%, respectively [21]. Slightly higher percentages of CV values are reported for periprosthetic BMD around hip and knee implants, with similar values of average precision error of about 3-4% [13, 15].

To our knowledge, no studies evaluated periprosthetic bone around TAR with DXA. Thus, as a preliminary step, the aim of our study is to determine precision of the DXA analysis of the distal tibia and talus with a dedicated scanning protocol.

Materials and methods

Study population and acquisition protocol

We included patients with TAR who were routinely sent to our department to perform a follow-up radiographic study. According to ISCD general guidelines, short-term precision was evaluated on 15 consecutive patients, with each ankle that was subsequently scanned three times both in the posteroanterior (PA) and lateral views [21]. All patients were repositioned after each scan. This prospective study was approved by the local ethics committee, and authorization for anonymized data publication was obtained. The study was conducted in accordance with the ethical standards of the 1964 Helsinki Declaration.

All DXA measurements and analysis were performed by an operator with seven years of experience in DXA using a Hologic QDR-Discovery W densitometer (Hologic Inc., Bedford, MA, USA). The periprosthetic BMD (in g/cm^2) was evaluated using the dedicated "metal removal" software algorithm, which is able to automatically exclude metal elements from the box analysis. In order to minimize the operator-related variability between serial analysis, the physician was not allowed to modify the bone area; the only possible operator intervention was the correction of software inaccuracies in metal exclusion.

The ankle joints of patients were scanned in both PA and lateral views. In order to reduce the position-related variability between scans, we developed a specific positioning protocol for both projections:

- the PA scan was acquired with the patient lying supine with the leg full-extended in slight internal rotation. Leg and foot were stabilized using the Hologic foot positioning device (the same used to perform the hip scan) [22]. This allowed for an internal rotation of about 20°, which is similar to that used for obtaining the "mortise" radiographic view, in which the entire ankle mortise is visible [23]. Mortise view is commonly included in the postoperative TAR radiographic assessment [3].

- for the lateral scan, the patient was turned on the side of the prosthesis until the ankle was laterally placed on the DXA table. The foot was dorsiflexed to position the plantar surface perpendicular to the lower leg, to prevent lateral rotation of the ankle. When necessary, a sandbag was placed on the forefoot to stabilize joint position. The hip positioning device was used to control dorsiflexion and keep the foot perpendicular to the leg.

The modality of ankle positioning for both posteroanterior and lateral views is shown in figures 1 and 2, respectively.

Regions of interest (ROI) placement

ROIs were located similarly to a previous radiographic study on TAR by Nodzo et al [24]. Four squared ROIs were placed in the periprosthetic bone in the PA and lateral images, two ROIs around the tibial implant (ROIs #1 and #2) and two ROIs just around the talar implants (ROIs #3 and #4). An additional ROI was placed in the lateral image to include the entire posterior calcaneal body (ROI #5). Finally, on each scan the software automatically placed a "*global*" ROI to include the overall bone area. To obtain the maximum reproducibility in ROI placement, we chose reference points on bone and prosthetic implants. Figures 3 and 4 show a detailed explanation of the procedure that we used to place each ROI on the PA and lateral scans. Once all ROI were defined, the software automatically copied onto the consecutive acquisitions using the *compare* tool present on the system. At this stage, the operator was able to check for adequate ROI placement.

Short-term Precision and Statistics

Short-term precision analysis was performed according to ISCD 2013 guidelines [21]. The BMD average value and standard deviation (SD) were calculated at each ROI. Then, we calculated the root mean square standard deviation (RMS-SD) of BMD. Coefficient of variation percentage (CV%) was calculated as the ratio between RMS-SD and the grand mean. The least significant change (LSC) at 95% confidence level was calculated as 2.77×CV; LSC represents the magnitude of BMD variation that needs to be exceeded at follow-up scan to represent a real biological change [25]. Reproducibility was calculated as the complement to 100% LSC. All calculations were performed using Microsoft Excel® (Microsoft, Redmond, WA) spreadsheet.

Results

Study population

A total of 15 patients was enrolled (7 males, 8 females) with a mean age of 57±12 years (mean±standard deviation) and a mean body mass index of 26±4 kg/m^2. Table 1 shows a summary of patients' characteristics including the type of prostheses that were implanted and the year of surgery, which ranged from 2013 to 2017. Etiology of ankle deformity was mainly related to post-traumatic osteoarthritis (13/15 cases, 86%), with one case of ankle instability (7%) and one case of rheumatoid arthritis (7%). All prostheses were implanted without bone cement. No surgery complications were presented at the moment of the study.

Short-term precision assessment

Table 2 and 3 show a general summary of periprosthetic short-term precision values (expressed as CV) for each ROI on PA and lateral scan respectively, including LSC and reproducibility values. The lateral projection showed lower mean CV values compared to the PA projection. In the PA scans, the average precision error was 3.34%, with the lowest value at the medial aspect of tibial side (ROI 1; CV = 2.77%). The highest CV value on PA scan was found on the medial aspect of talar side (ROI 3; CV= 4.89%). In the lateral projection, the average precision error was 2.21%, with the lowest value at the posterior calcaneal body (ROI 5; CV = 1.48%). The highest CV value on lateral scan was found on the posterior aspect of talar side (ROI 2; CV = 2,99%). Overall, the lowest precision error was found at both "*global*" ROIs, with a CV of 1.25% on the PA projection and 1.3% on the lateral projection. Both in the frontal and lateral projections the highest variability was found in the nearby of metallic implants (screws, plates). Figures 5 shows a DXA image (both PA and lateral scans) from one subjects of our study. The average time of each scan was less than a minute, and in general no patients referred excessive discomfort or was unable to complete the examination.

Discussion

To our knowledge, this is the first study that evaluated the short-term precision of periprosthetic BMD around TAR. In fact, the accuracy of BMD measurements in the periprosthetic bone around THA and TKA has been already comprehensively assessed in several studies [17, 19]. The main reason for the lack of data for TAR is that its use for the treatment of ankle arthritis was limited in the previous years by the high rate of complications of first generation implants [26]. Nevertheless, with recent advances in surgical instrumentation, techniques and design, ankle replacement showed better clinical outcomes, leading to longer survival of modern implants and increasing their use [27–29].

Previous studies evaluated the short-term reproducibility of the periprosthetic BMD measurements around THA and TKA. In 1995, Cohen and Rushton evaluated the accuracy of BMD measurement around THA, showing a mean precision error (expressed as CV) ranging from 2.7% to 3.4% [13]. Soininvaara and colleagues evaluated short-term BMD reproducibility around TKA in 30 patients with primary osteoarthrosis. In their study, the operated knee was measured twice in two projections, with BMD being evaluated at 9 different ROI [15]. The average precision error was 3.1% on femoral side and 2.9% on the tibial side, with the best precision (1.3%) corresponding to the femoral diaphysis above the implant and the poorest CV in patellar region (6.9%). Another study about TKA by Trevisan and colleagues showed that, with a dedicated analysis protocol, BMD CV% reproducibility ranged from 0.9% to 2.6% for the PA scan and from 2.7% to 5.6% for the lateral scan [30]. In our study we found very good reproducibility BMD values, that were consistent or even better to that of the abovementioned works.

Several factors can affect the reproducibility of BMD measurements, being patient positioning probably the most important. In fact, it has been showed that various degrees of femoral rotation have a significant impact on BMD measurements, suggesting that proper and reproducible positioning is necessary to improve BMD precision [31]. Similarly, Cohen and Rushton showed that femur rotation was the most significant factor that affected reproducibility when evaluating periprosthetic BMD after THA [13]. For this reason, we adopted a precise and dedicated patient positioning protocol, that was easy to reproduce and well tolerated by all patient. For this purpose, we used the same device used for foot positioning during hip scan, thus not requiring additional tools which may be expensive. In addition, by choosing fixed anatomic and prosthetic reference points, we ensured an easy and precise ROI relocation on all the scans. Regarding our results, we cannot exclude that performing the examination at a different degree of ankle rotation would have provided different BMD values: by using the same angle, we avoided this problem. Nevertheless, this aspect may be considered for setting the protocol of future longitudinal studies.

ROI size and heterogeneity of bone anatomy may also affect BMD reproducibility. Usually, the smaller the ROI, the greater the BMD variability [13, 15, 30, 32]. This is a well-known principle for DXA, which is also valid in clinical routine when measuring BMD at central sites. As an example, ISCD guidelines suggest to use total hip for serial BMD measurements, as this ROI is bigger than femoral neck ROI which is typically used for diagnostic purposes [33]. This was confirmed in our study, as global ROIs (which are the bigger in size) showed the highest reproducibility, while smallest ROIs (such as those at talar side on the PA projection) showed lowest reproducibility values. Similarly, ROI #2 on the PA projection was slightly less reproducible than ROI #1, a factor that is probably related to the concomitant presence of both tibia and fibula which complicates local anatomy.

The lateral projection showed better precision values compared to the PA acquisition. One reason may be that two of four ROIs of the PA scan (those at talar side) were smaller compared to those at tibial side, a factor that contributed to increase mean CV values. In addition, the lateral scan included a ROI in the calcaneus, which was larger than all other regions. Of note, calcaneus has the highest proportion of trabecular bone (which is reported to be >95%) [34, 35]. The BMD measured at other ROIs is mainly related to the amount of cortical bone, which is usually associated with slightly lower precision [32].

The main limitation of our study is that all scans were acquired with a single densitometer by a single operator, thus our results may not be directly transferable to operators with different experience and training, as well as to a different densitometer. Nevertheless, this source of variability may be limited by strictly applying the protocol that we detailed in our study.

In conclusion, our study showed that DXA can be used to precisely monitor bone density around ankle prostheses. Larger regions of interests were associated with lower

CV% values and better reproducibility. Further long-term longitudinal studies are required to assess the clinical utility of monitoring periprosthetic BMD around TAR with DXA, but careful patient positioning and precise ROI location are mandatory to obtain reliable results.

References

1. Nwachukwu BU, Bozic KJ, Schairer WW, et al (2015) Current Status of Cost Utility Analyses in Total Joint Arthroplasty: A Systematic Review. Clin Orthop Relat Res 473:1815–1827. doi: 10.1007/s11999-014-3964-4
2. Krause FG, Schmid T (2012) Ankle Arthrodesis versus Total Ankle Replacement. Foot Ankle Clin 17:529–543. doi: 10.1016/j.fcl.2012.08.002
3. Mulcahy H, Chew FS (2015) Current Concepts in Total Ankle Replacement for Radiologists: Features and Imaging Assessment. Am J Roentgenol 205:1038–1047. doi: 10.2214/AJR.14.14170
4. Chang C, Huang A, Palmer W (2015) Radiographic Evaluation of Hip Implants. Semin Musculoskelet Radiol 19:012–020. doi: 10.1055/s-0034-1396763
5. Cyteval C (2016) Imaging of knee implants and related complications. Diagn Interv Imaging 97:809–821. doi: 10.1016/j.diii.2016.02.015
6. Roth TD, Maertz NA, Parr JA, et al (2012) CT of the Hip Prosthesis: Appearance of Components, Fixation, and Complications. RadioGraphics 32:1089–1107. doi: 10.1148/rg.324115183
7. Fritz J, Lurie B, Potter HG (2015) MR Imaging of Knee Arthroplasty Implants. RadioGraphics 35:1483–1501. doi: 10.1148/rg.2015140216
8. Talbot BS, Weinberg EP (2016) MR Imaging with Metal-suppression Sequences for Evaluation of Total Joint Arthroplasty. RadioGraphics 36:209–225. doi: 10.1148/rg.2016150075

9. Espinosa N, Klammer G, Wirth SH (2017) Osteolysis in Total Ankle Replacement. Foot Ankle Clin 22:267–275. doi: 10.1016/j.fcl.2017.01.001

10. Yoon HS, Lee J, Choi WJ, Lee JW (2014) Periprosthetic osteolysis after total ankle arthroplasty. Foot ankle Int 35:14–21. doi: 10.1177/1071100713509247

11. Gaden MTR, Ollivere BJ (2013) Periprosthetic Aseptic Osteolysis in Total Ankle Replacement. Clin Podiatr Med Surg 30:145–155. doi: 10.1016/j.cpm.2012.10.006

12. Robertson DD, Mintzer CM, Weissman BN, et al (1994) Distal loss of femoral bone following total knee arthroplasty. Measurement with visual and computer-processing of roentgenograms and dual-energy x-ray absorptiometry. J Bone Joint Surg Am 76:66–76.

13. Cohen B, Rushton N (1995) Accuracy of DEXA measurement of bone mineral density after total hip arthroplasty. J Bone Joint Surg Br 77:479–83.

14. Guglielmi G, Muscarella S, Bazzocchi A Integrated imaging approach to osteoporosis: state-of-the-art review and update. Radiographics 31:1343–64. doi: 10.1148/rg.315105712

15. Soininvaara T, Kröger H, Jurvelin JS, et al (2000) Measurement of bone density around total knee arthroplasty using fan-beam dual energy X-ray absorptiometry. Calcif Tissue Int 67:267–72.

16. Cavalli L, Brandi ML (2014) Periprosthetic bone loss: diagnostic and therapeutic approaches. F1000Research 2:266. doi: 10.12688/f1000research.2-266.v2

17. Albanese C V, Santori FS, Pavan L, et al (2009) Periprosthetic DXA after total hip arthroplasty with short vs. ultra-short custom-made femoral stems. Acta Orthop 80:291–297. doi: 10.3109/17453670903074467

18. Merle C, Streit MR, Volz C, et al (2011) Bone remodeling around stable uncemented titanium stems during the second decade after total hip arthroplasty: a DXA study at 12 and 17 years. Osteoporos Int 22:2879–2886. doi: 10.1007/s00198-010-1483-z

19. Soininvaara T, Nikola T, Vanninen E, et al (2008) Bone mineral density and single photon emission computed tomography changes after total knee arthroplasty: a 2-year follow-up study. Clin Physiol Funct Imaging 28:101–106. doi: 10.1111/j.1475-097X.2007.00782.x

20. Soininvaara T, Miettinen H, Jurvelin J, et al (2004) Periprosthetic tibial bone mineral density changes after total knee arthroplastyOne-year follow-up study of 69 patients. Acta Orthop Scand 75:600–605. doi: 10.1080/00016470410001493

21. Schousboe JT, Shepherd JA, Bilezikian JP, Baim S (2013) Executive Summary of the 2013 International Society for Clinical Densitometry Position Development Conference on Bone Densitometry. J Clin Densitom 16:455–466. doi: 10.1016/j.jocd.2013.08.004

22. National Health and Nutrition Examination Survey (NHANES) (2007) Dual Energy X-ray Absorptiometry (DXA) Procedures Manual. Page 3-17. https://www.cdc.gov/nchs/data/nhanes/nhanes_07_08/manual_dexa.pdf. Accessed 23 Jan 2019

23. Long BW, Smith BJ, Merrill V Merrill’s atlas of radiographic positioning & procedures.

24. Nodzo SR, Miladore MP, Kaplan NB, Ritter CA (2014) Short to Midterm Clinical and Radiographic Outcomes of the Salto Total Ankle Prosthesis. Foot Ankle Int 35:22–29. doi: 10.1177/1071100713510497

25. El Maghraoui A, Achemlal L, Bezza A (2006) Monitoring of Dual-Energy X-ray Absorptiometry Measurement in Clinical Practice. J Clin Densitom 9:281–286. doi: 10.1016/j.jocd.2006.03.014

26. Lewis JS, Green CL, Adams SB, et al (2015) Comparison of First- and Second-Generation Fixed-Bearing Total Ankle Arthroplasty Using a Modular Intramedullary Tibial Component. Foot ankle Int 36:881–90. doi: 10.1177/1071100715576568

ACCEPTED MANUSCRIPT

27. Barg A, Zwicky L, Knupp M, et al (2013) HINTEGRA total ankle replacement: survivorship analysis in 684 patients. J Bone Joint Surg Am 95:1175–83. doi: 10.2106/JBJS.L.01234
28. Usuelli FG, Indino C, Maccario C, et al (2016) Total ankle replacement through a lateral approach: surgical tips. SICOT-J 2:38. doi: 10.1051/sicotj/2016029
29. Usuelli FG, Manzi L, Brusaferri G, et al (2017) Sagittal tibiotalar translation and clinical outcomes in mobile and fixed-bearing total ankle replacement. Foot Ankle Surg 23:95–101. doi: 10.1016/j.fas.2016.08.005
30. Trevisan C, Bigoni M, Denti M, et al (1998) Bone assessment after total knee arthroplasty by dual-energy X-ray absorptiometry: analysis protocol and reproducibility. Calcif Tissue Int 62:359–61.
31. Goh JC, Low SL, Bose K (1995) Effect of femoral rotation on bone mineral density measurements with dual energy X-ray absorptiometry. Calcif Tissue Int 57:340–3.
32. Bonnick S Lou (2010) Monitoring Changes in Bone Density. In: Bone Densitom. Clin. Pract. Humana Press, Totowa, NJ, pp 257–278
33. Baim S, Binkley N, Bilezikian JP, et al (2008) Official Positions of the International Society for Clinical Densitometry and executive summary of the 2007 ISCD Position Development Conference. J Clin Densitom 11:75–91. doi: 10.1016/j.jocd.2007.12.007
34. Bonnick S Lou (2010) Skeletal Anatomy in Densitometry. In: Bone Densitom. Clin. Pract. Humana Press, Totowa, NJ, pp 35–78
35. Peppler WT, Kim WJ, Ethans K, Cowley KC (2017) Precision of dual-energy X-ray absorptiometry of the knee and heel: methodology and implications for research to reduce bone mineral loss after spinal cord injury. Spinal Cord 55:483–488. doi: 10.1038/sc.2016.170

Acknowledgments

Authors' roles: CME contributed to study design, data acquisition, analysis and interpretation, manuscript drafting; FGU, CMA, CDS, DA and SG contributed to data acquisition and manuscript revising, LMS revised the manuscript and approved its final version.

CM is responsible for the integrity of the data analysis.

Figure 1. Patient positioning for the posteroanterior scan. All patients were lying supine with the leg full-extended. The Hologic device for hip positioning was used to obtain a slight internal rotation of about 15°-20° degree, similarly to the "mortise" radiographic view.

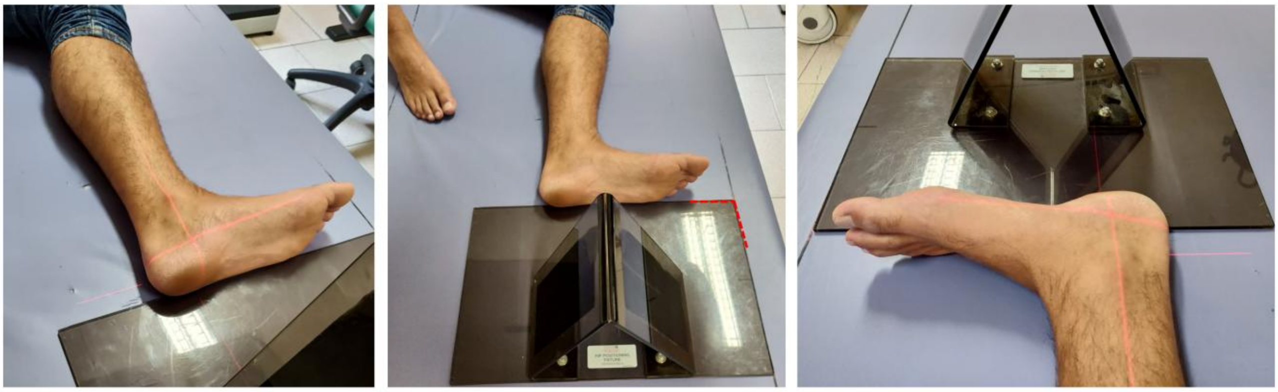

Figure 2. Patient positioning for the lateral scan. From the posteroanterior position, the patient was turned on the side of the prosthesis, so that the external part of the foot was in contact with the table. In order to position the plantar surface as perpendicular as possible to the lower leg, the Hologic device for hip positioning was used to support the plantar side of the foot. Of note, the external edge of the Hologic device was placed parallel to the table border, obtaining a right angle with the plantar surface of the foot (see red dashed line).

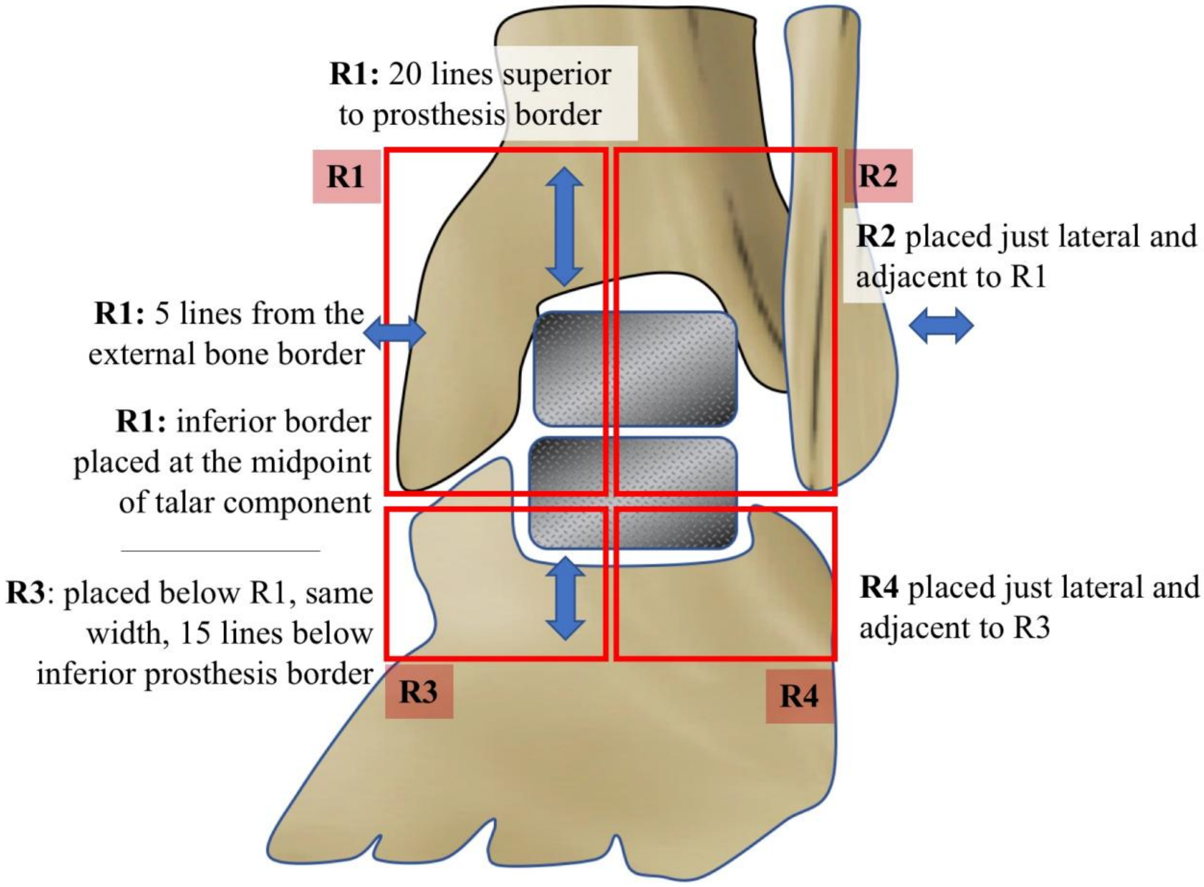

Figure 3. Detailed explanation of ROI placement on the posteroanterior scan. Four different ROIs were placed, two on the tibial side and two (slightly smaller) on the talar side.

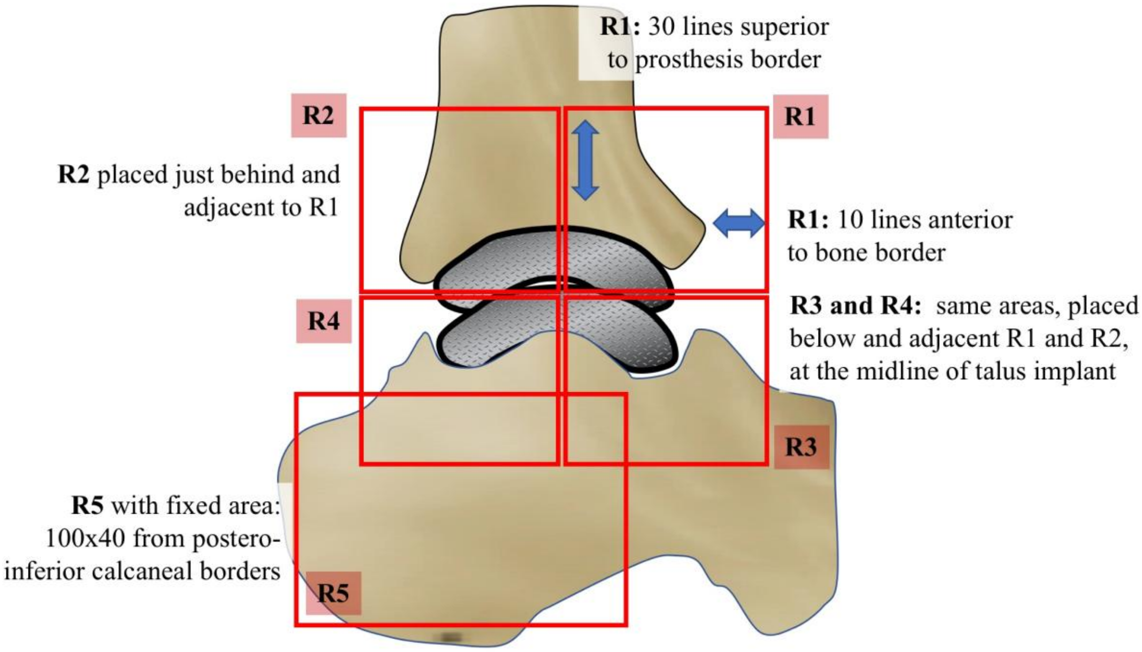

Figure 4. Detailed explanation of ROI placement on the lateral scan. Five different ROIs were placed, two on the tibial side, two (same dimension) on the talar side, plus a fifth ROI in the calcaneus.

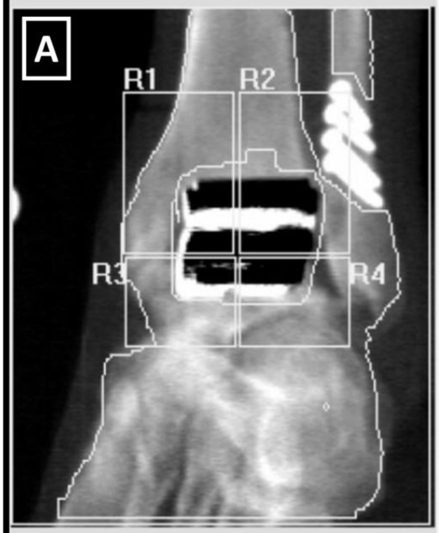

Region	Area[cm²]	BMC[(g)]	BMD[g/cm²]
GLOBAL	77.85	70.02	0.899
R1	7.69	6.72	0.874
R2	5.67	4.69	0.827
R3	5.15	5.36	1.040
R4	5.67	4.49	0.792
Net	24.18	21.25	0.879

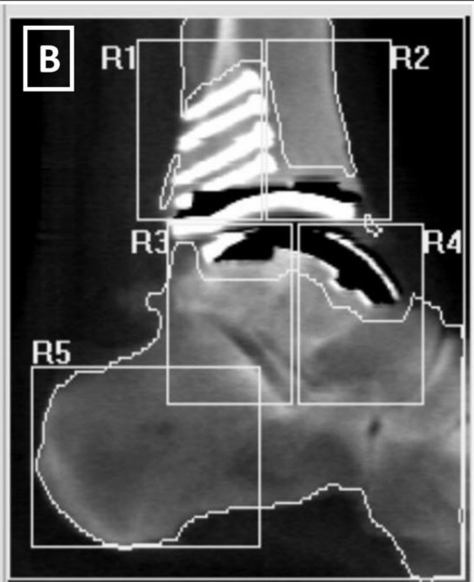

Region	Area[cm²]	BMC[(g)]	BMD[g/cm²]
GLOBAL	72.64	58.94	0.811
R1	2.57	2.58	1.002
R2	6.03	6.73	1.116
R3	11.76	12.67	1.077
R4	8.96	8.21	0.917
R5	23.24	14.12	0.607
Net	49.92	41.73	0.836

Figure 5. Example of periprosthetic DXA (A = posteroanterior scan, B = lateral scan) in a 70-years old patient with a Zimmer TM Ankle total ankle replacement, which was performed together with lateral fibular osteotomy (fixed with four metallic screws).

Table 1. A general overview of patients' characteristics including the type of prostheses, the year of surgery and osteoarthritis etiology. BMI= Body Mass Index; M=male; F=female

Patient n°	Gender	Age	BMI	Type of Prosthesis	Year of surgery	Osteoarthritis Aetiology
1	M	40	28.9	Zimmer TM ankle	2017	Post-traumatic
2	**F**	54	22.5	Zimmer TM ankle	2016	Post-traumatic
3	M	67	31.7	Zimmer TM ankle	2017	Post-traumatic
4	**F**	59	33.2	Hintegra	2016	Post-traumatic
5	M	70	29.7	Zimmer TM ankle	2017	Instability
6	M	77	25.2	Zimmer TM ankle	2017	Post-traumatic
7	F	48	27.7	Hintegra	2013	Post-traumatic
8	F	71	19.6	Zimmer TM ankle	2015	Post-traumatic
9	M	62	23.9	Zimmer TM ankle	2017	Post-traumatic
10	F	47	27.3	Zimmer TM ankle	2015	Rheumatoid Arthritis

11	F	46	22.4	Zimmer TM ankle	2017	Post-traumatic
12	F	68	23.0	Zimmer TM ankle	2017	Post-traumatic
13	M	56	24.0	Zimmer TM ankle	2017	Post-traumatic
14	M	37	30.1	Zimmer TM ankle	2016	Post-traumatic
15	F	60	30	Zimmer TM ankle	2017	Post-traumatic

Table 2. Summary of periprosthetic short-term precision values for each ROI in the posteroanterior scan, expressed as coefficient of variation (CV), with corresponding values of least significant change (LSC) and reproducibility. RMS SD = root mean square standard deviation.

Posteroanterior		**Tibial side**		**Talar side**		**Mean values**
	Global	**R1**	**R2**	**R3**	**R4**	
RMS SD	0.010	0.021	0.027	0.048	0.033	
CV	1.24%	2.77%	3.57%	4.89%	4.21%	3.34%
LSC	3.43%	7.68%	9.89%	13.54%	11.66%	9.24%
Reproducibility	96.57%	92.32%	90.11%	86.46%	88.34%	90.76%

Table 3. Summary of periprosthetic short-term precision values for each ROI in the lateral scan, expressed as coefficient of variation (CV), with corresponding values of least significant change (LSC) and reproducibility. RMS SD = root mean square standard deviation.

Lateral		**Tibial side**		**Talar side**		**Calcaneus**	**Mean values**
	Global	**R1**	**R2**	**R3**	**R4**	R5	
RMS SD	0.009	0.024	0.033	0.022	0.017	0.009	
CV	1.30%	2.59%	2.99%	2.73%	2.19%	1.48%	2.21%
LSC	3.61%	7.17%	8.30%	7.57%	6.06%	4.09%	6.13%
Reproducibility	96.39%	92.83%	91.70%	92.43%	93.94%	95.91%	93.87%